



HAL
open science

Chronology of Holocene storm events along the European Atlantic coast

Pierre Pouzet, Mohamed Maanan, Natalia Piotrowska, Agnès Baltzer, Pierre
Stéphan, Marc Robin

► **To cite this version:**

Pierre Pouzet, Mohamed Maanan, Natalia Piotrowska, Agnès Baltzer, Pierre Stéphan, et al.. Chronology of Holocene storm events along the European Atlantic coast: New data from the Island of Yeu, France. *Progress in Physical Geography*, 2018, 42 (4), pp.431-450. 10.1177/0309133318776500 . hal-01811916

HAL Id: hal-01811916

<https://hal.science/hal-01811916>

Submitted on 9 Jul 2020

HAL is a multi-disciplinary open access archive for the deposit and dissemination of scientific research documents, whether they are published or not. The documents may come from teaching and research institutions in France or abroad, or from public or private research centers.

L'archive ouverte pluridisciplinaire **HAL**, est destinée au dépôt et à la diffusion de documents scientifiques de niveau recherche, publiés ou non, émanant des établissements d'enseignement et de recherche français ou étrangers, des laboratoires publics ou privés.

Chronology of Holocene storm events along the European Atlantic coast: new data from the Island of Yeu, France

Pierre Pouzet^{1*}, Mohamed Maanan¹, Natalia Piotrowska², Agnes Baltzer¹, Pierre Stephan³, Marc Robin¹

¹ Université de Nantes LETG - UMR CNRS 6554, Nantes, France.

² Institute of Physics - CSE, Silesian University of Technology, Department of Radioisotopes, Gliwice, Poland.

³ Institut Universitaire Européen de la Mer, LETG - UMR CNRS 6554, Technopole Brest-Iroise, Plouzané, France.

* Corresponding author. E-mail: pierre.pouzet@univ-nantes.fr

Abstract

This paper reviews the reconstruction of European Atlantic storm events with the contribution of a new stormy reconstruction in its central part. Three marsh environments on the island of Yeu were chosen to identify disturbing storm events from the Mid- to Late Holocene with vibracore sampling, ¹⁴C dating and sedimentary analysis. Nine probable intervals of high energy deposition in these low transport activity environments are estimated: 600-500, near 1590, 2100-1950, 2850-2350, 3500-3270, 5400-5370, 6650-6510, near 7000 and between 7670 and 7470 cal y BP. By comparison with sedimentological paleostorm studies, we confirm six European Atlantic storm events estimated at near 600-300, 1700-1100, 2900-2500, 3500-3300, 5500-5100 and 7700-7100 BP, corresponding to worldwide Holocene cooling climatic periods. A comparison with other storminess reviews of worldwide main stormy coasts shows that Holocene storms can increase during global cooling periods in the northern hemisphere.

Keywords: Holocene, European coasts, storm events, climate change, sedimentology.

Highlights

Historical records of storm event reconstruction over a long period.

Evidence of storm events along the Atlantic coast is better preserved in coastal marshes.

Good correlation between storm episodes and cooling climatic periods.

1. Introduction

Numerous geological studies have rebuilt past Late Holocene landfalls in regions frequently struck by storms around the world (Jong et al., 2006; May et al., 2017; Osleger et al., 2009; Zhu et al., 2017), as in the North American continent which is the most studied area pursuing storminess analyses (Bennington and Farmer, 2014; Boldt et al., 2010; Das et al., 2013; Horwitz and Wang, 2005; Liu and Fearn, 1993, 2000; Mann et al., 2009; Mora et al., 2006; Parris et al., 2009). As the eastern United States is frequently struck by summer hurricanes, researchers tried to understand how the cyclonic season is correlated with global ocean-atmosphere mechanisms. Although only a few studies have focused on this recent issue, storminess reconstructions have also been developed for all other continents: Oceania (May et al., 2015, 2017; Nott and Hayne, 2001), Asia (Lallemand et al., 2015; Liu et al., 2001; Williams et al., 2015; Yu et al., 2009), Africa (Bozzano et al., 2002), South America (Oliveira et al., 2014; Ramírez-Herrera et al., 2012) and Mediterranean coasts (Degeai et al., 2015; Dezileau et al., 2011, 2016; Kaniewski et al., 2016; Sabatier et al., 2008, 2012; Vallve and Martin-Vide, 1998). Few studies have investigated the European Atlantic coast, where stormy chronologies are mainly concentrated on the British Isles (Hansom and Hall, 2009; Oldfield et al., 2010; Orme et al., 2015, 2016), and where some other works have recently analyzed Holocene French storms (Sorrel et al., 2009, 2012; Van Vliet Lanoe et al., 2014).

This paper focuses on the entire European Atlantic coast and has three main objectives: i) A proposal for the first overall chronology of storm events at the European coast scale, enabled by ii) The reconstruction of the stormy periods of the central part of the French Atlantic coast, the only flawed area missing for an overall European chronology; iii) A comparison of the general European Atlantic stormy dynamics with global climatic phases and other northern hemisphere storminess reviews. Only a few works extend to pre-5000 BP storminess observations, so we will propose new conclusions for the entire Holocene scale.

2. Material and methods

2.1. Study area

The study was conducted on the island of Yeu (Fig. 1). This island is very exposed to coastal flooding (Feuillet et al., 2012) and thus seems to be a relevant site for providing good markers of past European Atlantic extratropical storms. Stormy events mainly come from the ocean during the winter, and the number and the wind speed of these strong winter events in the whole of Europe have increased over several decades (Zappa et al., 2013). On the Atlantic coast, the sea level rise has been slowed since the last marine transgression ended nearly 7500 BP. In the area of the island of Yeu, a notable inflexion point is observed in sea-level curves (2.6 mm.yr⁻¹ of sea level increase before and 0.8 mm.yr⁻¹ after), testifying to relative coastline stabilization (Goslin et al., 2015; Stéphan and Goslin, 2014). We can thus obtain clues about past stormy events since the beginning of the Atlantic period.

Due to the north-eastern tilting of the island, the south-western coast is bordered by 7 to 23 m high cliffs, subjected to high marine erosion. In contrast, many sandy beaches predominate on the protected north-northwestern coast. Based on 2011 IGN LIDAR topography (Fig. 1), the island can be divided into two sections: a plain below 10 m NGF in the east and northeast of the island with the main coastal beaches and marsh, including our three coring sites, and a plateau above 10-15 m NGF covering the west-southwest lands. According to the *Service Hydrographique et Océanographique de la Marine* (SHOM), the French Atlantic coast has a semi-diurnal tidal regime and the highest tidal ranges are around 5.5 to 6 meters.

For this study, we chose three northern marshes that had not been humanly impacted before the 19th century. This choice was guided by the naturalness of the environment and its natural evolution (Pottier and Robin, 1997). As in other central western France coastal areas (Pouzet

et al., 2015), urbanization started recently on the island of Yeu in the mid-20th century so that only the first few centimeters of the three cores have been disturbed by human activity. The first station is the Marais de la Guerche, forming a small basin probably formerly connected to the sea by a northwest outlet. This built-up environment is composed by a sandy beach with a few houses, roads and vegetation between the coastline and the marsh. The marsh is made up of a Holocene sedimentary filling, 3 to 4 m thick, in an old valley carved in gneiss-type metamorphic rocks (from BRGM geological map). The profile shows the location of the Yeu-MG core. The second station is an old water stream bed, called the Coulee Verte. The paleo-river, drilled approximately 150 m from the coastline, leads to a small sandy bay surrounded by rocks. The profile shows this very narrow valley carved in gneiss-type rocks with sedimentary material that can reach 4 m of thickness. The last station is the Marais de la Croix, which is situated in the southeast of the island of Yeu, 300 m from the southern rocky coast and the northern sandy beaches. The profile of the southern coastline towards the north shoreline over a kilometer shows the overall shape of the island, which slopes gently northward with a slight depression in the center carved into the gneiss. The profile crosses an old valley slightly incised in the rocky substrate. It also shows the sand dunes that cover the northern coast, which explain the filling of the mouths of the small valleys and the backward development of the marshes.

2.2. Sampling and sediment analysis

Coring sediments were sampled using an Eijkelkamp 50 mm Ø, motor-driven percussion corer in three coastal deposit environments: a 250 cm deep core at the Marais de la Guerche, a 300 cm deep core at the Coulee Verte and a 180 cm deep core at the Marais de la Croix (Fig. 1). Core positions were surveyed using a Trimble Differential Global Positioning System (DGPS). All locations were linked to geo-referenced IGN (French National Geographic

Institute) benchmarks and leveled with respect to the NGF datum (French leveling datum, linked to the Mean Sea Level at Marseille, France) during the Peps-Mer 2015 mission. A measure of core compaction has been made in the field to precise the vertical positioning of the samples. Cores were covered in 1-m long plastic tubes and cut into half-cylinders with a plastic film sealing. Cores have been stored at +4°C to slow down deposits oxidation. Sediments were characterized by a visual litho-microstratigraphic analysis, to identify major changes in granulometry, color, organic matter and to identify each macrofossil observed. We then analyzed reworked levels to avoid possible confusions in sample dating.

Possible sources of altitudinal error were considered in detail by Shennan, 1986a, 1986b. Overall altitudinal error was evaluated at ± 0.14 m, accounting for (i) a potential ± 0.02 m uncertainty in the measurement of the stratigraphic position of the sample and (ii) a ± 0.12 m uncertainty due to leveling to the benchmark.

The sediment cores were cut into slices of approximately 1 cm, then dried in a streamer at between 35 and 40°C. The prepared samples were burned at 500°C in a 1 L muffle furnace for four hours, in order to assess the organic matter content by the loss in the ignition process (Santisteban et al., 2004). Grain size was measured with a laser granulometer (Malvern Mastersizer 2000). Sedimentological high-resolution elemental analyses were evaluated using an Avaatech© XRF core scanner at the EOPC laboratory (Bordeaux). Element intensities were normalized by the total intensity (count per second of each spectrum: cps) (Bouchard et al., 2011; Martin et al., 2014). Three type of elements were conserved for this study to interpret geochemical data: two proved marine elements (Calcium: Ca and Strontium: Sr), two mixed indicators (Silicon: Si, with a marine dominating tendencies and Zinc: Zn, continental dominating tendencies) and two last continental proxies (Iron: Fe and Titanium: Ti) (Bozzano

et al., 2002; Chagué-Goff et al., 2012, 2017; Das et al., 2013; Degeai et al., 2015; Naquin et al., 2014; Pouzet et al., 2018 (submitted)).

Eleven samples were dated in the Gliwice Radiocarbon Laboratory center of the Silesian University of Technology, Gliwice, Poland, by the accelerator mass spectrometry (AMS) technique. Samples of high organic matter content were selected based on the LOI percentages (peat or organic sediment), and a well formed *Bittium reticulatum* shell was found in the sandy layer of the La Guerche core. Organic samples were subjected to standard preparation to extract total organic carbon, which included treatment with 0.5 M hydrochloric acid, washing in demineralized water and drying. Combustion to CO₂ was performed in an elemental analyzer (EA) for peat and organic-rich samples, or in an infra-red furnace in oxygen flow for sediment samples with lower carbon content (Piotrowska, 2013). Graphitization took place in an automated graphitization system AGE-3 (Wacker et al., 2010). Determinations of ¹⁴C content were carried out in the Direct AMS laboratory, Bothell, USA (Zoppi, 2010).

3. Results and discussion

3.1. Dating and age-depth modeling

Radiocarbon ages were calibrated using the IntCal13 curve (Reimer et al., 2013) or the NH1 curve (Hua et al., 2013) except for the shell sample. For the latter, the Marine13 curve was used and the local reservoir effect of -12 ± 38 yrs was added, averaging the 5 nearest available data from the Marine Correction Database (<http://calib.qub.ac.uk/marine/>) points, based on Tisnérat-Laborde et al., 2010. The results were introduced into OxCal software v.4.2.4 (Bronk Ramsey, 2009) and the *P_Sequence* algorithm (Bronk Ramsey, 2008) was used to obtain the age-depth relationships for the three investigated cores (see Fig. 2). The collection year 2015

AD was included at the depth of 0 cm, and the models were extrapolated to reach the depths of 194 cm (Marais de la Guerche), 279 cm (Coulee Verte), and 97 cm (Marais de la Croix). For the most intensively dated core of Marais de la Guerche, it was possible to introduce the boundaries at the most significant lithological changes at 13, 55 and 155 cm. The overall agreement indices for the three sequences were 93% (Marais de la Guerche), 87% (Coulee Verte) and 98% (Marais de la Croix), confirming the good performance of the models. The scarcity of samples for two cores resulted in considerably higher model uncertainties (see Fig. 2). Nevertheless, the ages were calculated for each centimeter in the core to provide information about the timing of recorded environmental changes.

3.2. Lithostratigraphy analysis of the island of Yeu

The base of the Coulee Verte core (YEU-CV) is dated after 7280 cal y BP (275 cm). This paleo-river functioned as a river until 6200 cal y BP (235 cm). The grain size shows coarser sand grains than the current sediments, with sand levels reaching an average of 50% and low OM content. Both marine and continental elements were higher than actually as the river carried continental sediments when it was connected by the sea. (Fig. 3). The river system forms a seaward-prograding, tide-dominated estuarine delta (silts sediments with an OM evolution), which has been gradually filling the estuary since 6400 cal y BP. These facies, interrupted by a major event dated at 5302 cal y BP (183 cm) bringing a 3-cm diameter pebble, are bounded by prominent flooding surfaces that record landward shifts in environments, with a general gradual grain size and marine elements decreases and OM and continentals elements increases. The accelerated filling of the river after the most important storm events closed the estuary system between 3500 and 3300 cal y BP. Since this period, the system has functioned as a marsh system until today, with higher OM proportions (at least 40%) and a silty-clayey type mean grain size. Higher values of Zn, Fe and Ti are opposed to

low Ca, Sr and Si elements. A last main disturbance is reported in this recent horizon near centimeter 100, increasing the OM rate from 40 to 60% at centimeter 80.

The lithostratigraphy of the second core (YEU-MG) is mainly composed by peat, interrupted by a huge 40 centimeter wide sandy sheet (Fig. 4). A strong event seems to have deeply impacted the Marais de la Guerche, with a marine sandy layer observed from centimeter 10 to 51 in this peaty environment. The marine occurrence is confirmed by the presence of *Bittium reticulatum*, which is dated at 1800 cal y BP at centimeter 37, and their high Ca, Si and Sr values. The sharp contact between the lower peat and the marine layer testifies to the suddenness of the event. It was produced by two consecutive increases in sand, enhancing the mean grain size. The onset of these two increases is estimated at 2070 and 1940 cal y BP. Before 2100 cal y BP, the main peaty composition of this core from a “closed from the sea environment” enables the detection of numerous sandy allochthonous arrivals to its base, dated at nearly 8000 cal y BP at centimeter 200. A series of disturbing events is recorded between centimeters 70 and 82, where high grain size, geochemical and OM variations are observed. A slight impacting storminess can be observed near centimeter 120 (fall in OM and increase in sand level, with a Sr peak), in contrast to the major disturbance reported at centimeter 170 and estimated at 5370 y cal BP (peaks in Si, Ca, Sr and fall of Fe). The major impact of this event is recorded by OM content, with a strong increase estimated from 10 to 80%. The last facies observed shows a large grain size and geochemical variation near the rocky basis (centimeter 175 to 200), when the lagoon was still connected to the sea.

The Marais de La Croix core (YEU-MC) shows fewer storminess signals because of its greater distance from the coastline, making overwash traces less graphically significant than those of the other two sites (Fig. 5). This core is also shorter than the others, with a base estimated at 3000 cal y BP near centimeter 100. At the bottom of the core, the environment is

more energetic, with coarse sediments low OM levels (10 to 20%), and slight geochemical variations to 55 cm. Several storm events can be detected in this lower dynamic sheet with numerous grain size, Ca and Sr increases and OM variations. An important event disturbs the environment near 2100 – 1950 cal y BP (50-55 cm). After this stormy period, there is a change in the environment with a lower energetic depositional marsh with marked increases in OM (30 to 50%), Zn, Fe and notable mean grain size, Si and Sr decreases, until the top of the core. However, this upper section is interrupted by another significant storm deposit near 25 cm, dated at 550 cal y BP, with OM levels dropping to 15-20% and massively increasing coarser grains (5 to 50% of sand). A slight increase of Ca, Sr and Si is also observed, with a fall of Zn. A last geochemical signal of storminess is also reported in the upper part of the core (cm.8), corresponding to a post 2010 AD date. Radiocarbon dating may not allow a precise and recent estimation of this event.

3.3. French Atlantic storm evidence under climate change

Overall, nine periods of storminess increases, called Yeu Stormy Periods (YSPs), can be distinguished in the three investigated cores (Fig. 6). We then correlated them with European paleo-environment studies from the scientific literature to confirm these series of events on a climatic chronological scale.

The latest storm event reported is YSPa (Fig. 6). It disturbed the island of Yeu environment from 600 to 550 cal y BP at the beginning of the “Little Ice Age”. YSPa matches a French 721-603 cal y BP high storm period (Degeai et al., 2015), in an overall European high storminess event from 600 to 300 cal y BP (Sorrel et al., 2012). In northern Europe, a British climatic deterioration started between 700 and 550 cal y BP (Devoy et al., 1996; Hansom and

Hall, 2009; Oldfield et al., 2010; Wilson et al., 2004), resulting in a large period of sand mobilization (692-504 cal y BP, Gilbertson et al., 1999), and a 580-470 cal y BP Welsh peak of storminess (Orme et al., 2015). There was also a 650 cal y BP Spanish stormy period in southern Europe (Dezileau et al., 2016). No storminess was detected there during the “Medieval Warm Period”.

At the beginning of the “Medieval Dark Age” cold climatic period, we report a 1590 cal y BP storminess (YSPb; Fig. 6). Bao et al., 1999 described a lagoon breaching near 1600 cal y BP at Albufeira, Portugal, stating that a “*dramatic opening of the tidal inlet provoked a significant change in the sedimentation regime*”. This breach happened when this part of the country was experiencing a “*transgressive dune building period from strong wind activity with sandy invasion*” according to Clarke and Rendell, 2006. In France, a storm event was reported near 1550 cal y BP (Van Vliet Lanoe et al., 2014) in a 1950-1050 cal y BP period of increased storm activity (Sabatier et al., 2012), and more widely in a 1900-1050 cal y BP northern coastal European period of high storminess (Sorrel et al., 2012). There are reports in other countries of two 1560-1550 cal y BP Welsh (Orme et al., 2015) and 1650-1450 cal y BP Croatian (Kaniewski et al., 2016) peaks of storminess, and a 1530 cal y BP Scottish period of sand drift (Gilbertson et al., 1999) in a 1620-1470 cal y BP erosional period corresponding to climatic deterioration (Oldfield et al., 2010). YEU-CV shows that the YSPb period may have ended the disturbance of the leading huge nearly-Anno Domini event.

Before this “Medieval Dark Age”, the “Roman Warm Period” underwent a storm event (YSPc: 2100-1950 cal y BP; Fig. 6) which deeply disturbed the island, found at 55 cm deep at YEU-MG and YEU-MC and at 100 cm deep at YEU-CV. It corresponds to a high OM increase for YEU-CV and YEU-MC, and to the sharp contact between a coarse sand (mean grain size of 331 μm) and a peaty layer (22 μm) in YEU-MG. Two peaty samples are dated

before (860 cal y BP at 8 cm) and after (2063 cal y BP at 52 cm) the sandy layer. This storm series opened a large breach in the La Guerche marsh, which functioned as a permanent inlet for 1200 years. The entire European coast underwent deep storm impacts similar to those estimated in the island of Yeu near Anno Domini. Degeai et al., 2015 observed a high Mediterranean stormy period in southern France between 2044 and 1993 cal y BP. A storm event was also reported in Brittany at 2060 cal y BP by Van Vliet Lanoe et al. (2014). Peaks of storminess have been reported from 2090 to 1970 cal y BP in western Wales (Orme et al., 2015). Lastly, a more coastal morphological approach mentions the start of a transgressive dune building period at 2200 cal y BP due to strong wind activity with sand invasion in central western Portugal (Clarke and Rendell, 2006).

In the Late Subboreal Bronze and Iron Ages, YSPd and YSPe can be traced in the island of Yeu cores from 2850 to 2350 cal y BP (corresponding to a “Iron Age Cold Period”) and from 3500 to 3270 cal y BP, probably during a “Piora Oscillation” (Lamb, 1995) (Fig. 6). With its 500 years interval, YSPd (2850-2350 cal y BP) shows around twenty matches, including half with French storm events: 2470 cal y BP (Baltzer et al., 2014), 2570-2507 cal y BP (Degeai et al., 2015), 2600-2300 cal y BP (Regnaud, 1999), 2460 cal y BP (Regnaud et al., 1995, 1996), 2800-2400 cal y BP (Sabatier et al., 2012), 2700 cal y BP (Sorrel et al., 2009), 2700 and 2350 cal y BP (Van Vliet Lanoe et al., 2014). Other periods of increasing storminess are reported in Sweden: 2800-2200 cal y BP (Jong et al., 2006), Spain: 2300 cal y BP (Dezileau et al., 2016), Scotland and Northern Ireland: 2800-2400 cal y BP (Orme et al., 2016), Wales: 2840-2800 cal y BP (Orme et al., 2015), Croatia: 3400-2550 cal y BP (Kaniewski et al., 2016) and on a wider scale in northern coastal Europe: 3300-2400 cal y BP (Sorrel et al., 2012). Two dune mobilization periods are also reported, one due to high aeolian activity starting at 2750 cal y BP in Denmark (Clemmensen et al., 2009) and the other linked to climatic deterioration between 3100 and 2400 cal y BP in Northern Ireland (Wilson et al., 2004).

Lastly, this YSPd event is correlated with two so-called Scottish (from 2950 cal y BP, (Oldfield et al., 2010) and Spanish (between 2600 and 2300 cal y BP, (Rodríguez-Ramírez et al., 1996) erosional periods. For YSPe (3500-3270 cal y BP), mainly French correlations are obtained: a 3500 cal y BP storm event (Van Vliet Lanoe et al., 2014); a massive 3350 cal y BP sand mobilization at the base of the Pilat dune in a high dune development period from a severe storm increase 4000-3000 years ago (Clarke et al., 2002); two 3400-2550 and 3650-3200 cal y BP periods of increased Mediterranean storm activity (Kaniewski et al., 2016; Sabatier et al., 2012); and two Atlantic coastal marshes covered by the sea (3400-3020 cal y BP and 3600-3155 cal y BP, Visset and Bernard, 2006). We also notice in northern Europe a 3300 cal y BP British period of increased storm activity (Orme et al., 2016) or notable sand drift (3800-3300 cal y BP, Gilbertson et al., 1999), and a 3400 cal y BP notable Dutch storm surge (Jelgersma et al., 1995).

During the “Atlantic” Holocene period, two other large sand incursions seriously disturbed the island of Yeu (Fig. 6). The first event is assessed from 5400 to 5370 cal y BP (YSPf) and the second from 6650 to 6510 cal y BP (YSPg). Gilbertson et al., 1999 confirms these occurrences with two notable Scottish sand drifts for 5380 cal y BP and 6605 cal y BP. We also report a high dune mobilization period due to climatic deterioration from 6900 to 5500 cal y BP, and the start of a dune net erosion event from 5400 cal y BP in Northern Ireland (Wilson et al., 2004). Finally, the two oldest events, 7000 cal y BP YSPh and 7570-7470 cal y BP YSPi, may be uncertain because these stormy periods are detected near the contact of the rocky orthogenesis core bases (Fig. 3 and 4). Only a few European paleostorm works focus on the Mid- to Early Holocene, so we note fewer correlations with a French 7150 cal y BP storm event (Van Vliet Lanoe et al., 2014) and a Scottish 7470 cal y BP notable sand drift in a 7500-7000 cal y BP period of sand incursions (Gilbertson et al., 1999).

3.4. Proposal for an overall chronological reconstruction of storm events at the European level, and comparison with global data

Only a few works have focused on the chronology of stormy periods near the European Atlantic coast. Jackson et al., 2005 extracted seven Holocene “windy episodes” from the grain size analysis of an Iceland core; these are reported in Fig. 7A. Orme et al., 2016 (in Fig. 7 of this reference) carried out a general analysis of a storminess chronology for the British Isles since 4000 BP from several previous regional studies. We extracted six stormy periods (Fig. 7B) from this work based on the reconstruction of storminess from the Outer Hebrides, Scotland, from sand influx into a peaty environment (Orme et al., 2016); numerous Scottish and Northern Irish studies showing phases of sand transport (dunes or wedges) (Dawson et al., 2004; Gilbertson et al., 1999; Sommerville et al., 2003; Tisdall et al., 2013; Wilson et al., 2004); Cliff Top Storm Deposits from Shetland sites, Scotland (Hansom and Hall, 2009), and the minerogenic input into a Cairngorms lake, Scotland, reflecting climate deterioration phases (Oldfield et al., 2010). Based on these references summarized in Figure 7 of Orme et al., 2016, we extracted periods of 3400-3100 cal y BP, 2700-2400 cal y BP, 1800 cal y BP, 1550 cal y BP, 1200-1100 cal y BP and 800-300 cal y BP as crossed-works of major storminess in Britain. As Atlantic French storms generally pass through France in a SW-NE direction, we reported Sorrel et al., 2009 storm results (from Fig. 9) for northwestern France (Fig. 7C). Baltzer et al., 2014 and Van Vliet Lanoe et al. (2014) also obtained numerous stormy periods for the last 9000 years from two Brittany (France) sedimentary studies, reported in Fig. 7D. The last two chronologies found in our region were extracted from storminess linked to dune construction in Aquitaine, France (Fig. 7F), and western central Portugal in Fig. 7G (Clarke et al., 2002; Clarke and Rendell, 2006). It is important to note that these last two references are less precise for storminess analysis because they focus mainly on dune building, but they are the only ones available for the southern European Atlantic coast.

To complete this regional-scale analysis, the French Atlantic stormy periods found in this study are recorded in Fig. 7E. As a storm can't impact both northern and southern Atlantic coasts in the same time, data discussed here testify storminess increasing periods and assess tendencies for the Holocene evolution of storm activity. This work can't expose the precise historical storms variation in the entire European Atlantic scale in which northern and southern comparisons should not be acceptable.

From this comparison, we can extract several periods of European Atlantic Storm Events (EASEs) in which most of these references note enhanced storminess (Fig. 7). Six main EASE periods are clearly observed: 600-300 BP (EASE 1), 1700-1100 BP (EASE 2), 2900-2400 BP (EASE 3), 3500-3300 BP (EASE 4), 5500-5100 BP (EASE 5) and 7700-7100 BP (EASE 6). Another questionable EASE can be reported around 2000 BP, but we cannot be sure about including it because only Van Vliet Lanoe et al., 2014 shows it, correlated with the start of a Portuguese dune building period (Clarke and Rendell, 2006). In general, the overall stormy periods compared in Fig. 7 are well correlated between the northern and central Atlantic coast, but the Portuguese data show slightly divergent conclusions, with periods sometimes not linked to all the northern studies. Consequently, northern and central European storminess may diverge from the southern one. However, this can also be discussed with the construction of dune building, the main topic of Clarke and Rendell, 2006, which cannot record precisely high past storm activity. Finally, before 4000 BP, only a few European studies provide clues to detect further EASEs, so only the Late to Mid-Holocene period can be assessed. For the Early Holocene, there are fewer matches because most sedimentological paleostorm studies focus on the Early to Mid-Holocene, until nearly 4000 BP.

We have added global data at the bottom of this graph (Fig. 7I) from Wanner et al., 2011 who determined worldwide Holocene cold events from numerous previous works. The main study

used by Wanner et al., 2011 and recorded in their Fig. 3, is a standardized ocean stacked ice rafted debris (IRD) from Bond et al., 1997, 2001. The latter results are also presented here (Fig. 7II) and testify to occurrences of cold climatic periods estimated during the Holocene (numbered from 0 to 6 in Fig. 7II).

We can conclude that the extracted EASE 1, 2 and 3 match with Wanner's Holocene cold events. Every EASE is also linked to a high record of ice rafted debris associated with a cold ocean-atmosphere linked period, a so-called Bond event. We can observe an increase in storminess during the early "Little Ice Age" (EASE 1), the "Medieval Dark Age" (EASE 2), an "Iron Age Cold Period" (EASE 3), and during other earlier Mid-Holocene cold periods (EASE 4 to 6). Consequently, a net relationship can be detected between cold periods and European Atlantic storms.

Although storms come from other dynamics elsewhere in the world, we compared this cooling influence hypothesis with five other Holocene storminess reviews carried out in the northern hemisphere. Our conclusion follows Mediterranean storm studies for Mid- to Late Holocene (Degeai et al., 2015; Dezileau et al., 2011, 2016, Sabatier et al., 2008, 2012; Vallve and Martin-Vide, 1998), reviewed by Kaniewski et al., 2016 (Fig. 7H). We then added to Fig. 7I the results of Swedish storminess detection made by Jong et al., 2006 as the North Sea can also be impacted by storms in the European continent. A correlation with the evolution of global temperatures is also possible. However, these studies are limited to the last 5000 years, and only a few works extend to the Early Holocene for long-trend storminess observations. We thus completed our global analyses with three long-term Holocene studies made in the three other high stormy oceanic basins. Noren et al., 2002 (Fig. 7J), Osleger et al., 2009 (Fig. 6K) and Zhu et al., 2017 (Fig. 7L) showed that the Western Atlantic coast and all the Pacific Ocean can also follow the hypothesis of an increase in storminess during Holocene cooling

periods. This comparison show that all previous oceanic basin scale reviews made in the northern hemisphere underline more frequent stormy impacts when the climate was cooler than average in the last 10 000 years.

4. Conclusion

Based on sedimentary analyses, we have identified nine possible paleostorm events in three Yeu Island deposition environments. Using OM levels, geochemical signals, sand proportion and grain size signatures, we have characterized a 2100-1950 cal y BP (YSPc) interval as a deeply storm-disturbed period, five other major impacted periods (YSPa: 600-500 cal y BP, YSPd: 2850-2350 cal y BP, YSPe: 3500-3270 cal y BP, YSPf: 5400-5370 cal y BP and YSPg: 6650-6510 cal y BP), and three periods with a less meaningful storminess hypothesis near 1590 cal y BP (YSPb), 7000 cal y BP (YSPh), and between 7670 and 7470 cal y BP (YSPi).

On the European Atlantic coast, six stormy periods stand out from the last 8000 years: 600-300 BP (EASE 1), 1700-1100 BP (EASE 2), 2900-2500 BP (EASE 3), 3500-3300 BP (EASE 4), 5500-5100 BP (EASE 5) and 7700-7100 BP (EASE 6) corresponding to Mid- to Late Holocene global cold events (Bond et al., 1997, 2001; Wanner et al., 2011). With the comparison made in the entire northern hemisphere, our results follow the hypothesis of an increase in Holocene storminess during global cooling periods.

5. Acknowledgments

Analyses, operating costs and field measurements were funded by the Fondation de France (research program « *Reconstitution des événements climatiques extrêmes à l'aide des multi-indicateurs* ») and OR2C-AXIS 3 (part of the OSUNA program and the Pays-de-la-Loire region). We are grateful to the town hall of the island of Yeu for helping us with fieldwork.

The authors gratefully acknowledge Isabelle Billy and her sedimentary core technical team of the EPOC (University of Bordeaux 1) for XRF spectrometric core scanner analysis. The authors gratefully acknowledge editor Dr. B. Yarnal and two anonymous reviewers for their useful comments, which help us to greatly improve this article.

6. References

- Baltzer A, Walter-Simonnet A-V, Mokeddem Z, et al. (2014) Climatically-driven impacts on sedimentation processes in the Bay of Quiberon (south Brittany, France) over the last 10,000 years. *The Holocene*: 679–688. DOI: 10.1177/0959683614526933.
- Bao R, Freitas M da C and Andrade C (1999) Separating eustatic from local environmental effects: a late-Holocene record of coastal change in Albufeira Lagoon, Portugal. *The Holocene* 9(3): 341–352. DOI: 10.1191/095968399675815073.
- Bennington JB and Farmer EC (2014) Recognizing Past Storm Events in Sediment Cores Based on Comparison to Recent Overwash Sediments Deposited by Superstorm Sandy. In: *Learning from the Impacts of Superstorm Sandy*. Academic Press, pp. 89–106.
- Boldt KV, Lane P, Woodruff JD, et al. (2010) Calibrating a sedimentary record of overwash from Southeastern New England using modeled historic hurricane surges. *Marine Geology* 275(1–4): 127–139. DOI: 10.1016/j.margeo.2010.05.002.
- Bond G, Showers W, Cheseby M, et al. (1997) A Pervasive Millennial-Scale Cycle in North Atlantic Holocene and Glacial Climates. *Science* 278(5341): 1257–1266. DOI: 10.1126/science.278.5341.1257.
- Bond G, Kromer B, Beer J, et al. (2001) Persistent Solar Influence on North Atlantic Climate During the Holocene. *Science* 294(5549): 2130–2136. DOI: 10.1126/science.1065680.
- Bouchard F, Francus P, Pienitz R, et al. (2011) Sedimentology and geochemistry of thermokarst ponds in discontinuous permafrost, subarctic Quebec, Canada. *Journal of Geophysical Research: Biogeosciences* 116(G2): G00M04. DOI: 10.1029/2011JG001675.
- Bozzano G, Kuhlmann H and Alonso B (2002) Storminess control over African dust input to the Moroccan Atlantic margin (NW Africa) at the time of maxima boreal summer insolation: a record of the last 220 kyr. *Palaeogeography, Palaeoclimatology, Palaeoecology* 183(1–2): 155–168. DOI: 10.1016/S0031-0182(01)00466-7.
- Bronk Ramsey C (2008) Deposition models for chronological records. *Quaternary Science Reviews* 27(1–2). INTegration of Ice-core, Marine and Terrestrial records (INTIMATE): Refining the record of the Last Glacial-Interglacial Transition: 42–60. DOI: 10.1016/j.quascirev.2007.01.019.
- Bronk Ramsey C (2009) Bayesian Analysis of Radiocarbon Dates. *Radiocarbon* 51(1): 337–360. DOI: 10.2458/azu_js_rc.51.3494.

- Chagué-Goff C, Andrew A, Szczuciński W, et al. (2012) Geochemical signatures up to the maximum inundation of the 2011 Tohoku-oki tsunami — Implications for the 869 AD Jogan and other palaeotsunamis. *Sedimentary Geology* 282. The 2011 Tohoku-oki tsunami: 65–77. DOI: 10.1016/j.sedgeo.2012.05.021.
- Chagué-Goff C, Szczuciński W and Shinozaki T (2017) Applications of geochemistry in tsunami research: A review. *Earth-Science Reviews* 165: 203–244. DOI: 10.1016/j.earscirev.2016.12.003.
- Clarke M, Rendell H, Tastet J-P, et al. (2002) Late-Holocene sand invasion and North Atlantic storminess along the Aquitaine Coast, southwest France. *The Holocene* 12(2): 231–238. DOI: 10.1191/0959683602h1539r.
- Clarke ML and Rendell HM (2006) Effects of storminess, sand supply and the North Atlantic Oscillation on sand invasion and coastal dune accretion in western Portugal. *The Holocene* 16(3): 341–355. DOI: 10.1191/0959683606h1932rp.
- Clemmensen LB, Murray A, Heinemeier J, et al. (2009) The evolution of Holocene coastal dunefields, Jutland, Denmark: A record of climate change over the past 5000 years. *Geomorphology* 105(3–4): 303–313. DOI: 10.1016/j.geomorph.2008.10.003.
- Das O, Wang Y, Donoghue J, et al. (2013) Reconstruction of paleostorms and paleoenvironment using geochemical proxies archived in the sediments of two coastal lakes in northwest Florida. *Quaternary Science Reviews* 68: 142–153. DOI: 10.1016/j.quascirev.2013.02.014.
- Dawson A, Elliott L, Noone S, et al. (2004) Historical storminess and climate ‘see-saws’ in the North Atlantic region. *Marine Geology* 210(1–4). Storms and their significance in coastal morpho-sedimentary dynamics: 247–259. DOI: 10.1016/j.margeo.2004.05.011.
- Degeai J-P, Devillers B, Dezileau L, et al. (2015) Major storm periods and climate forcing in the Western Mediterranean during the Late Holocene. *Quaternary Science Reviews* 129: 37–56. DOI: 10.1016/j.quascirev.2015.10.009.
- Devoy RJN, Delaney C, Carter RWG, et al. (1996) Coastal Stratigraphies as Indicators of Environmental Changes upon European Atlantic Coasts in the Late Holocene. *Journal of Coastal Research* 12(3): 564–588.
- Dezileau L, Sabatier P, Blanchemanche P, et al. (2011) Intense storm activity during the Little Ice Age on the French Mediterranean coast. *Palaeogeography Palaeoclimatology Palaeoecology / Palaeogeography Palaeoclimatology and Palaeoecology* 299(1–2): 289–297. DOI: 10.1016/j.palaeo.2010.11.009.
- Dezileau L, Pérez-Ruzafa A, Blanchemanche P, et al. (2016) Extreme storms during the last 6,500 years from lagoonal sedimentary archives in Mar Menor (SE SPAIN). *Climate of the Past Discussions*: 1–36. DOI: 10.5194/cp-2016-20.
- Feuillet T, Chauveau É and Pourinet L (2012) Xynthia est-elle exceptionnelle ? Réflexions sur l'évolution et les temps de retour des tempêtes, des marées de tempête, et des risques de surcotes associés sur la façade atlantique française. *Norôis* n° 222(1): 27–44.
- Gilbertson DD, Schwenninger J-L, Kemp RA, et al. (1999) Sand-drift and Soil Formation Along an Exposed North Atlantic Coastline: 14,000 Years of Diverse Geomorphological, Climatic and

- Human Impacts. *Journal of Archaeological Science* 26(4): 439–469. DOI: 10.1006/jasc.1998.0360.
- Goslin J, Van Vliet Lanoe B, Spada G, et al. (2015) A new Holocene relative sea-level curve for western Brittany (France): Insights on isostatic dynamics along the Atlantic coasts of north-western Europe. *Quaternary Science Reviews* 129: 341–365. DOI: 10.1016/j.quascirev.2015.10.029.
- Hansom JD and Hall AM (2009) Magnitude and frequency of extra-tropical North Atlantic cyclones: A chronology from cliff-top storm deposits. *Quaternary International* 195(1–2). Hurricanes and Typhoons: From the Field Records to the Forecast: 42–52. DOI: 10.1016/j.quaint.2007.11.010.
- Horwitz MH and Wang P (2005) Sedimentological Characteristics and Internal Architecture of Two Overwash Fans From Hurricanes Ivan and Jeanne. *Géology Faculty Publications*.
- Hua Q, Barbetti M and Rakowski AZ (2013) Atmospheric Radiocarbon for the Period 1950–2010. *Radiocarbon* 55(4): 2059–2072. DOI: 10.2458/azu_js_rc.55.16177.
- Jackson MG, Oskarsson N, Trønnnes RG, et al. (2005) Holocene loess deposition in Iceland: Evidence for millennial-scale atmosphere-ocean coupling in the North Atlantic. *Geology* 33(6): 509–512. DOI: 10.1130/G21489.1.
- Jelgersma S, Stive MJF and van der Valk L (1995) Holocene storm surge signatures in the coastal dunes of the western Netherlands. *Marine Geology* 125(1): 95–110. DOI: 10.1016/0025-3227(95)00061-3.
- Jong R de, Björck S, Björkman L, et al. (2006) Storminess variation during the last 6500 years as reconstructed from an ombrotrophic peat bog in Halland, southwest Sweden. *Journal of Quaternary Science* 21(8): 905–919. DOI: 10.1002/jqs.1011.
- Kaniewski D, Marriner N, Morhange C, et al. (2016) Solar pacing of storm surges, coastal flooding and agricultural losses in the Central Mediterranean. *Scientific Reports* 6: 25197. DOI: 10.1038/srep25197.
- Lallemant S, Lehu R, Rétif F, et al. (2015) A ~ 3000 years-old sequence of extreme events revealed by marine and shore deposits east of Taiwan. *Tectonophysics*. DOI: 10.1016/j.tecto.2015.11.001.
- Lamb HH (1995) *Climate, History and the Modern World*. 2 edition. London: Routledge.
- Liu K and Fearn ML (1993) Lake-sediment record of late Holocene hurricane activities from coastal Alabama. *Geology* 21(9): 793–796. DOI: 10.1130/0091-7613(1993)021<0793:LSROLH>2.3.CO;2.
- Liu K and Fearn ML (2000) Reconstruction of Prehistoric Landfall Frequencies of Catastrophic Hurricanes in Northwestern Florida from Lake Sediment Records. *Quaternary Research* 54(2): 238–245. DOI: 10.1006/qres.2000.2166.
- Liu K, Shen C and Louie K (2001) A 1,000-Year History of Typhoon Landfalls in Guangdong, Southern China, Reconstructed from Chinese Historical Documentary Records. *Annals of the Association of American Geographers* 91(3): 453–464. DOI: 10.1111/0004-5608.00253.
- Mann ME, Woodruff JD, Donnelly JP, et al. (2009) Atlantic hurricanes and climate over the past 1,500 years. *Nature* 460(7257): 880–883. DOI: 10.1038/nature08219.

- Martin L, Mooney S and Goff J (2014) Coastal wetlands reveal a non-synchronous island response to sea-level change and a palaeostorm record from 5.5 kyr to present. *The Holocene* 24(5): 569–580. DOI: 10.1177/0959683614522306.
- May SM, Brill D, Engel M, et al. (2015) Traces of historical tropical cyclones and tsunamis in the Ashburton Delta (north-west Australia). *Sedimentology* 62(6): 1546–1572. DOI: 10.1111/sed.12192.
- May SM, Brill D, Leopold M, et al. (2017) Chronostratigraphy and geomorphology of washover fans in the Exmouth Gulf (NW Australia) – A record of tropical cyclone activity during the late Holocene. *Quaternary Science Reviews* 169: 65–84. DOI: 10.1016/j.quascirev.2017.05.023.
- Mora C, Miller D and Grissino-Mayer H (2006) Tempest in a tree ring: Paleotempestology and the record of past hurricanes. *The Sedimentary Record* 4(3): 4.
- Naquin JD, Liu K, McCloskey TA, et al. (2014) Storm deposition induced by hurricanes in a rapidly subsiding coastal zone. *Journal of Coastal Research*: 308–313. DOI: 10.2112/SI70-052.1.
- Noren AJ, Bierman PR, Steig EJ, et al. (2002) Millennial-scale storminess variability in the northeastern United States during the Holocene epoch. *Nature* 419(6909): 821–824. DOI: 10.1038/nature01132.
- Nott J and Hayne M (2001) High frequency of ‘super-cyclones’ along the Great Barrier Reef over the past 5,000 years. *Nature* 413(6855): 508–512. DOI: 10.1038/35097055.
- Oldfield F, Battarbee RW, Boyle JF, et al. (2010) Terrestrial and aquatic ecosystem responses to late Holocene climate change recorded in the sediments of Lochan Uaine, Cairngorms, Scotland. *Quaternary Science Reviews* 29(7–8): 1040–1054. DOI: 10.1016/j.quascirev.2010.01.007.
- Oliveira FM, Macario KD, Simonassi JC, et al. (2014) Evidence of strong storm events possibly related to the little Ice Age in sediments on the southern coast of Brazil. *Palaeogeography, Palaeoclimatology, Palaeoecology* 415. Continental and Coastal Marine Records of Centennial to Millennial Changes in South American Climate since the Last Glacial Maximum: 233–239. DOI: 10.1016/j.palaeo.2014.03.018.
- Orme LC, Davies SJ and Duller G a. T (2015) Reconstructed centennial variability of Late Holocene storminess from Cors Fochno, Wales, UK. *Journal of Quaternary Science* 30(5): 478–488. DOI: 10.1002/jqs.2792.
- Orme LC, Reinhardt L, Jones RT, et al. (2016) Aeolian sediment reconstructions from the Scottish Outer Hebrides: Late Holocene storminess and the role of the North Atlantic Oscillation. *Quaternary Science Reviews* 132: 15–25. DOI: 10.1016/j.quascirev.2015.10.045.
- Osleger DA, Heyvaert AC, Stoner JS, et al. (2009) Lacustrine turbidites as indicators of Holocene storminess and climate: Lake Tahoe, California and Nevada. *Journal of Paleolimnology* 42(1): 103–122. DOI: 10.1007/s10933-008-9265-8.
- Parris AS, Bierman PR, Noren AJ, et al. (2009) Holocene paleostorms identified by particle size signatures in lake sediments from the northeastern United States. *Journal of Paleolimnology* 43(1): 29–49. DOI: 10.1007/s10933-009-9311-1.

- Piotrowska N (2013) Status report of AMS sample preparation laboratory at GADAM Centre, Gliwice, Poland. *Nuclear Instruments and Methods in Physics Research Section B Beam Interactions with Materials and Atoms* 294. DOI: 10.1016/j.nimb.2012.05.017.
- Pottier P and Robin M (1997) L'île d'Yeu, un espace convoité : développement et aménagement. *Mappemonde, revue internationale de cartographie* (1–1997): 18–23.
- Pouzet P, Creach A and Godet L (2015) Dynamique de la démographie et du bâti dans l'ouest du Marais poitevin depuis 1705. *Norois. Environnement, aménagement, société* (234): 83–96. DOI: 10.4000/norois.5589.
- Pouzet P, Maanan M, Schmidt S, et al. (2018) Three centuries of historical and geological data for the marine deposit reconstruction: examples from French Atlantic coast. *Marine Geology* (submitted).
- Ramírez-Herrera M-T, Lagos M, Hutchinson I, et al. (2012) Extreme wave deposits on the Pacific coast of Mexico: Tsunamis or storms? — A multi-proxy approach. *Geomorphology* 139–140: 360–371. DOI: 10.1016/j.geomorph.2011.11.002.
- Regnaud H (1999) L'élévation et les variations du niveau marin à l'Holocène terminal dans l'Ouest français : une approche par les dépôts de tempêtes [Sea-level elevation and variation during late holocene in western France ; storm surge relicts as indicators]. *Quaternaire* 10(2): 181–188. DOI: 10.3406/quate.1999.1641.
- Regnaud H, Cocaign J-Y, Saliege J-F, et al. (1995) Mise en évidence d'une continuité temporelle dans la constitution de massifs dunaires du Sud-Boréal (3600 BP) à l'Actuel sur le littoral septentrional de la Bretagne: un exemple dans l'Anse du Verger (Ille-et-Vilaine). *Comptes rendus de l'Académie des sciences. Série 2. Sciences de la terre et des planètes* 321(4): 303–310.
- Regnaud H, Jennings S, Delaney C, et al. (1996) Holocene sea-level variations and geomorphological response: An example from northern Brittany (France). *Quaternary Science Reviews* 15(8). L. Ortlieb: 781–787. DOI: 10.1016/S0277-3791(96)00070-4.
- Reimer PJ, Bard E, Bayliss A, et al. (2013) IntCal13 and Marine13 Radiocarbon Age Calibration Curves 0–50,000 Years cal BP. *Radiocarbon* 55(4): 1869–1887. DOI: 10.2458/azu_js_rc.55.16947.
- Rodríguez-Ramírez A, Rodríguez-Vidal J, Cáceres L, et al. (1996) Recent coastal evolution of the Doñana National Park (SW Spain). *Quaternary Science Reviews* 15(8). L. Ortlieb: 803–809. DOI: 10.1016/S0277-3791(96)00068-6.
- Sabatier P, Dezileau L, Condomines M, et al. (2008) Reconstruction of paleostorm events in a coastal lagoon (Hérault, South of France). *Marine Geology* 251(3–4): 224–232. DOI: 10.1016/j.margeo.2008.03.001.
- Sabatier P, Dezileau L, Colin C, et al. (2012) 7000 years of paleostorm activity in the NW Mediterranean Sea in response to Holocene climate events. *Quaternary Research* 77(1): 1–11. DOI: 10.1016/j.yqres.2011.09.002.
- Santisteban JI, Mediavilla R, López-Pamo E, et al. (2004) Loss on ignition: a qualitative or quantitative method for organic matter and carbonate mineral content in sediments? *Journal of Paleolimnology* 32(3): 287–299. DOI: 10.1023/B:JOPL.0000042999.30131.5b.

- Shennan I (1986a) Flandrian sea-level changes in the Fenland. I: The geographical setting and evidence of relative sea-level changes. *Journal of Quaternary Science* 1(2): 119–153. DOI: 10.1002/jqs.3390010204.
- Shennan I (1986b) Flandrian sea-level changes in the Fenland. II: Tendencies of sea-level movement, altitudinal changes, and local and regional factors. *Journal of Quaternary Science* 1(2): 155–179. DOI: 10.1002/jqs.3390010205.
- Sommerville AA, Hansom JD, Sanderson DCW, et al. (2003) Optically stimulated luminescence dating of large storm events in Northern Scotland. *Quaternary Science Reviews* 22(10–13). LED 2002: 1085–1092. DOI: 10.1016/S0277-3791(03)00057-X.
- Sorrel P, Tessier B, Demory F, et al. (2009) Evidence for millennial-scale climatic events in the sedimentary infilling of a macrotidal estuarine system, the Seine estuary (NW France). *Quaternary Science Reviews* 28(5–6): 499–516. DOI: 10.1016/j.quascirev.2008.11.009.
- Sorrel P, Debret M, Billeaud I, et al. (2012) Persistent non-solar forcing of Holocene storm dynamics in coastal sedimentary archives. *Nature Geoscience* 5(12): 892–896. DOI: 10.1038/ngeo1619.
- Stéphan P and Goslin J (2014) Holocene relative sea-level rise along the atlantic and English Channel coasts of france: reassessment of existing data using ‘sea-level index points’ method. *Quaternaire* 25(4): 295–312.
- Tisdall EW, McCulloch RD, Sanderson DCW, et al. (2013) Living with sand: A record of landscape change and storminess during the Bronze and Iron Ages Orkney, Scotland. *Quaternary International* 308–309. Geoarchaeology: a toolbox of approaches applied in a multidisciplinary research discipline: 205–215. DOI: 10.1016/j.quaint.2013.05.016.
- Tisnérat-Laborde N, Paterne M, Métivier B, et al. (2010) Variability of the northeast Atlantic sea surface $\Delta 14C$ and marine reservoir age and the North Atlantic Oscillation (NAO). *Quaternary Science Reviews* 29(19–20). DOI: 10.1016/j.quascirev.2010.06.013.
- Vallve MB and Martin-Vide J (1998) Secular Climatic Oscillations as Indicated by Catastrophic Floods in the Spanish Mediterranean Coastal Area (14th–19th Centuries). *Climatic Change* 38(4): 473–491. DOI: 10.1023/A:1005343828552.
- Van Vliet Lanoe B, Goslin J, Hallégouet B, et al. (2014) Middle- to late-Holocene storminess in Brittany (NW France): Part I - morphological impact and stratigraphical record. *Holocene* 24(4): 413–433. DOI: 10.1177/0959683613519687.
- Visset L and Bernard J (2006) Évolution du littoral et du paysage, de la presqu’île de Rhuy à la rivière d’Étel (Massif armoricain – France), du Néolithique au Moyen Âge. *ArcheoSciences. Revue d’archéométrie* (30): 143–156. DOI: 10.4000/archeosciences.315.
- Wacker L, Němec M and Bourquin J (2010) A revolutionary graphitisation system: Fully automated, compact and simple. *Nuclear Instruments and Methods in Physics Research Section B Beam Interactions with Materials and Atoms* 268(7): 931–934. DOI: 10.1016/j.nimb.2009.10.067.
- Wanner H, Solomina O, Grosjean M, et al. (2011) Structure and origin of Holocene cold events. *Quaternary Science Reviews* 30(21–22): 3109–3123. DOI: 10.1016/j.quascirev.2011.07.010.
- Williams H, Choowong M, Phantuwongraj S, et al. (2015) Geologic Records of Holocene Typhoon Strikes on the Gulf of Thailand Coast. *Marine Geology*. DOI: 10.1016/j.margeo.2015.12.014.

- Wilson P, McGourty J and Bateman MD (2004) Mid-to late-Holocene coastal dune event stratigraphy for the north coast of Northern Ireland. *The Holocene* 14(3): 406–416. DOI: 10.1191/0959683604hl716rp.
- Yu K-F, Zhao J-X, Shi Q, et al. (2009) Reconstruction of storm/tsunami records over the last 4000 years using transported coral blocks and lagoon sediments in the southern South China Sea. *Quaternary International* 195(1–2): 128–137. DOI: 10.1016/j.quaint.2008.05.004.
- Zappa G, Shaffrey LC, Hodges KI, et al. (2013) A Multimodel Assessment of Future Projections of North Atlantic and European Extratropical Cyclones in the CMIP5 Climate Models. *Journal of Climate* 26(16): 5846–5862. DOI: 10.1175/JCLI-D-12-00573.1.
- Zhu Z, Feinberg JM, Xie S, et al. (2017) Holocene ENSO-related cyclic storms recorded by magnetic minerals in speleothems of central China. *Proceedings of the National Academy of Sciences of the United States of America* 114(5): 852–857. DOI: 10.1073/pnas.1610930114.
- Zoppi U (2010) Radiocarbon AMS Data Analysis: From Measured Isotopic Ratios to ^{14}C Concentrations. *Radiocarbon* 52(1): 165–170.

PRE-PRINT

Table 1. Sample details, results of AMS radiocarbon dating and calibration for the island of Yeu

Lab. ID	Sample name/depth	Material	Age BP/pMC	Calibrated age
GdA-4719	YEU-MG-A/10 cm	peat	950 ± 30	68.2% probability 920 BP (18.1%) 900 BP 870 BP (37.6%) 825 BP 815 BP (12.6%) 800 BP 95.4% probability 925 BP (95.4%) 795 BP
GdA-4720	YEU-MG-B/37 cm	<i>Bittium reticulatum</i> marine shell	2190 ± 25	68.2% probability 1860 BP (68.2%) 1735 BP 95.4% probability 1920 BP (95.4%) 1680 BP
GdA-4721	YEU-MG-C/54 cm	peat	2080 ± 30	68.2% probability 2105 BP (16.3%) 2085 BP 2065 BP (51.9%) 2000 BP 95.4% probability 2140 BP (94.5%) 1990 BP 1960 BP (0.9%) 1950 BP
GdA-4722	YEU-MG-D/150 cm	peat	3725 ± 35	68.2% probability 4145 BP (17.7%) 4120 BP 4100 BP (16.8%) 4070 BP 4045 BP (33.6%) 3990 BP 95.4% probability 4225 BP (2.0%) 4205 BP 4160 BP (93.4%) 3975 BP
GdA-4723	YEU-MG-E/188 cm	organic sediment	6570 ± 25	68.2% probability 7480 BP (68.2%) 7435 BP 95.4% probability 7555 BP (3.2%) 7545 BP 7510 BP (92.2%) 7430 BP
GdA-4724	YEU-MC-A/14 cm	peat	106.28 ± 0.38	68.2% probability 2005.2 AD (68.2%) 2007.7 AD 95.4% probability 1956.8 AD (1.9%) 1957.2 AD 2004.8 AD (93.5%) ...
GdA-4725	YEU-MC-B/52 cm	organic sediment	1865 ± 25	68.2% probability 1865 BP (15.5%) 1845 BP 1830 BP (39.7%) 1780 BP 1760 BP (13.1%) 1740 BP 95.4% probability 1870 BP (95.4%) 1730 BP
GdA-4726	YEU-CV-A/5 cm	humus	111.08 ± 0.43	68.2% probability 1995.9 AD (68.2%) 1998.1 AD 95.4% probability 1957.3 AD (3.7%) 1958 AD 1995.2 AD (91.7%) 1999.1 AD
GdA-4727	YEU-CV-B/94 cm	organic sediment	1925 ± 20	68.2% probability 1895 BP (50.6%) 1865 BP 1845 BP (17.6%) 1830 BP 95.4% probability 1925 BP (5.9%) 1910 BP 1900 BP (89.5%) 1825 BP
GdA-4728	YEU-CV-C/186 cm	organic sediment	4580 ± 25	68.2% probability 5435 BP (7.3%) 5423 BP

				5320 BP (57.2%) 5289 BP 5155 BP (3.7%) 5146 BP 95.4% probability 5445 BP (12.3%) 5415 BP 5325 BP (63.4%) 5280 BP 5165 BP (10.8%) 5135 BP 5110 BP (8.8%) 5075 BP
GdA-4729	YEU-CV-D/261 cm	organic sediment	5930 ± 30	68.2% probability 6790 BP (66.4%) 6720 BP 6701 BP (1.8%) 6698 BP 95.4% probability 6845 BP (6.5%) 6815 BP 6800 BP (88.9%) 6670 BP

PRE-PRINT

Figure 1. Cartography of the island of Yeu with the three coring sites, based on 2013 IGN BD ORTHO and 2011 IGN LIDAR topography.

Figure 2. Age-depth models obtained using the OxCal P_Sequence algorithm for the 3 investigated sites.

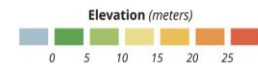
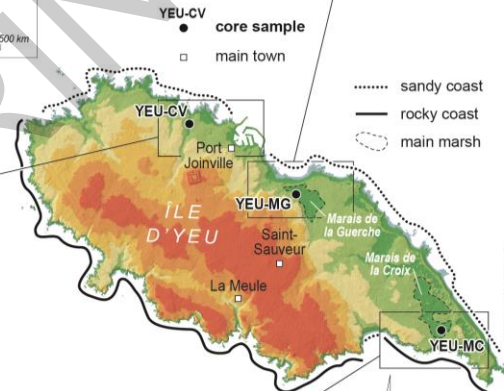
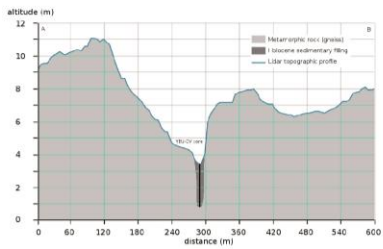
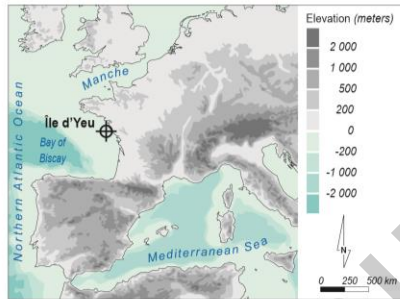
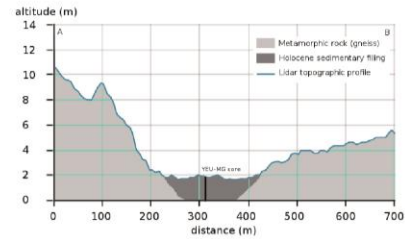
Figure 3. Log and lithostratigraphic interpretation of the Coulée Verte core.

Figure 4. Log and lithostratigraphic interpretation of the Marais de la Guerche core.

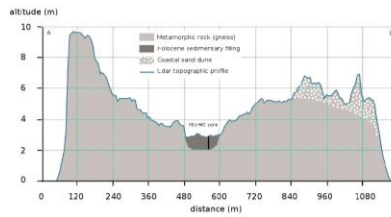
Figure 5. Log and lithostratigraphic interpretation of the Marais de la Croix core.

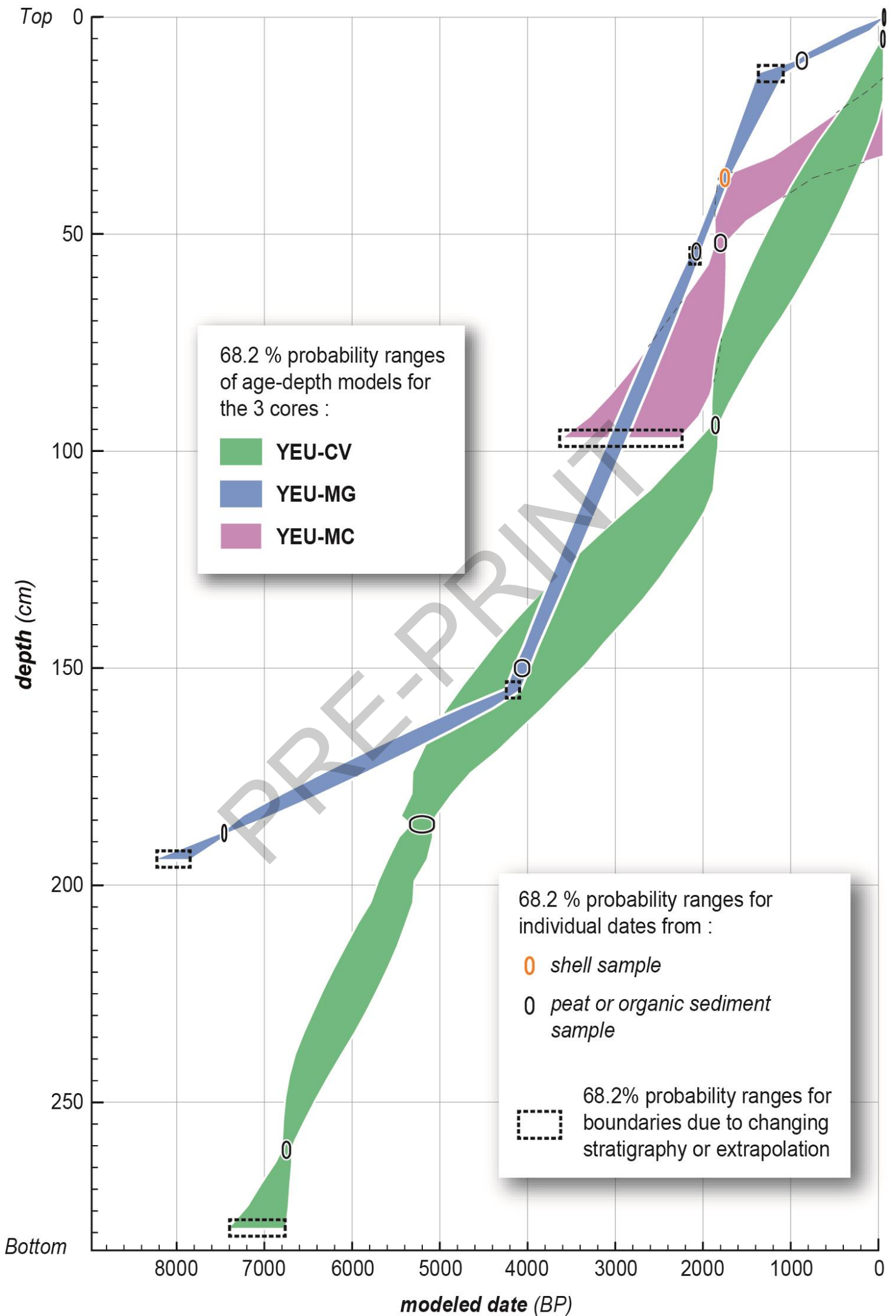
Figure 6. Determination of Yeu Stormy Periods (YSPs) by comparing the five storm indicators: mean grain size, OM content, sand level, Ca and Sr normalized geochemical elements measured in the three different cores.

Figure 7. Proposition of European Atlantic Storm Events (EASEs) extracted from the comparison of existing European Atlantic storminess studies from sedimentary analysis. A: Iceland (Jackson et al., 2005); B: Brittany islands (Orme et al., 2016); C: Normandy (Sorrel et al., 2009); D: Brittany (Baltzer et al., 2014; Van Vliet Lanoe et al., 2014); E: Western-central France (this paper); F: Aquitaine (Clarke et al., 2002); and G: Central Portugal (Clarke and Rendell, 2006). Correlation of EASEs extracted from this work with I: global high cold climatic periods (Wanner et al., 2011) determined from II: standardized ocean stacked Ice Rafted Debris records, with Bond events numbered (Bond et al., 2001, 1997; Wanner et al., 2011).



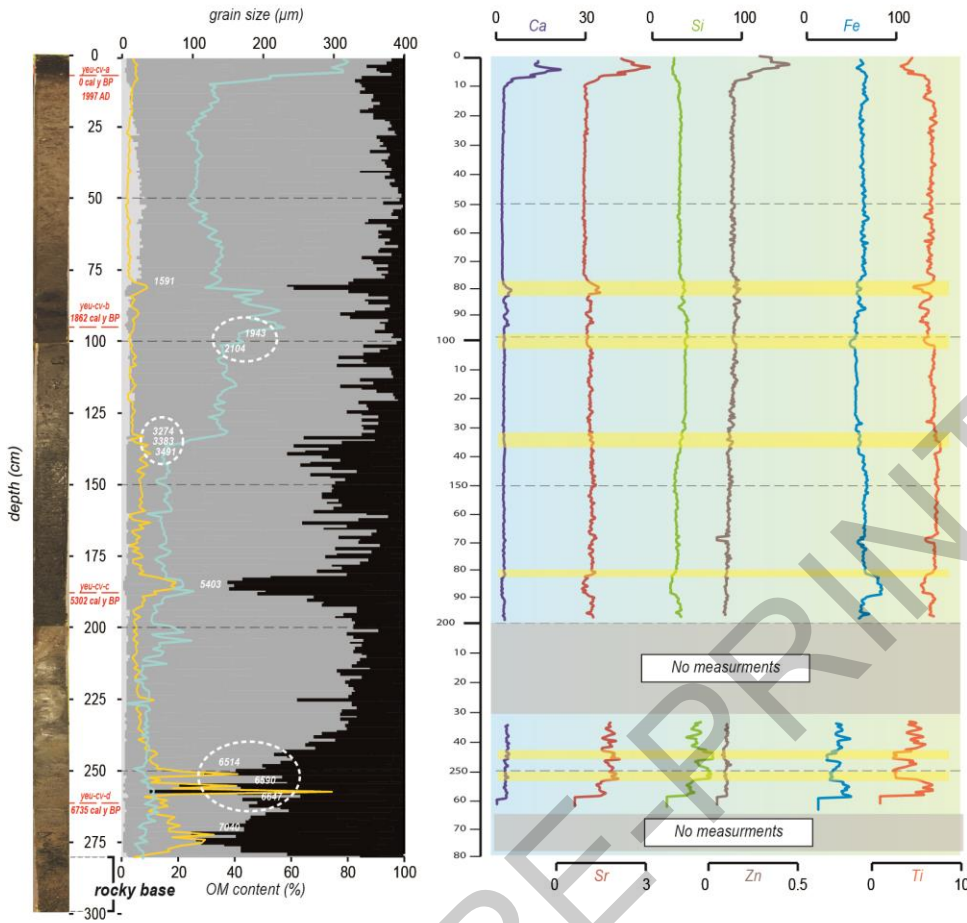
Sources : IGN BD ORTHO (2013), IGN LIDAR topography (2011)



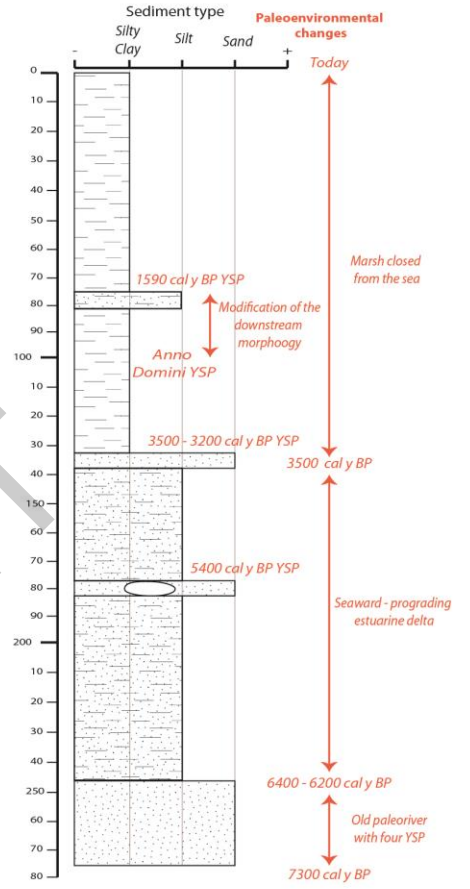


Coulée Verte (YEU-CV)

Data obtained from sedimentary analyses



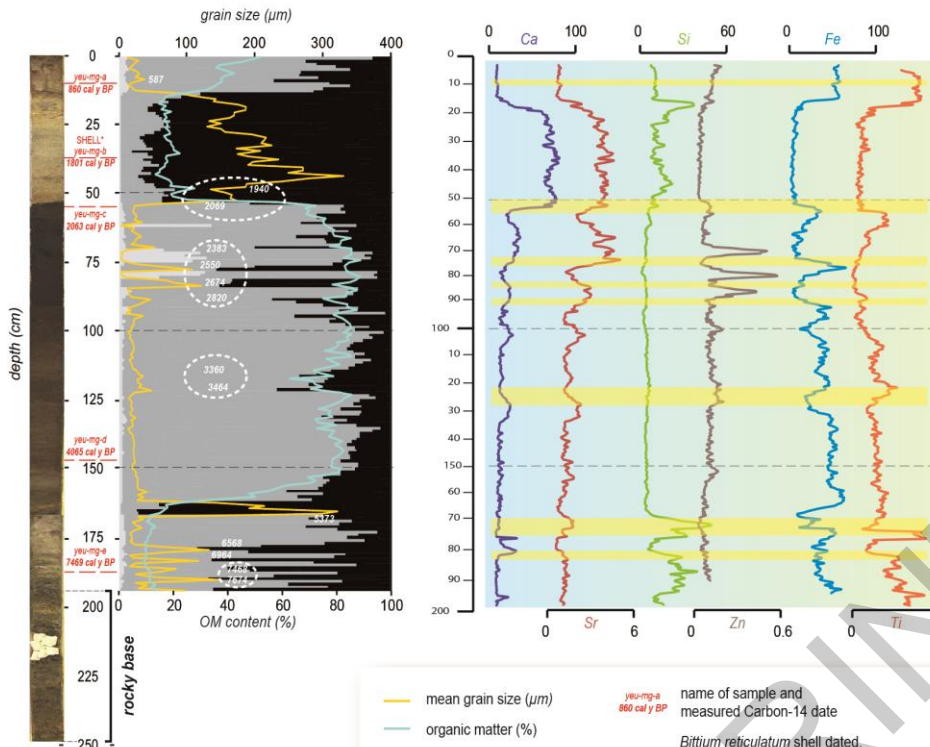
Interpretation of the lithostratigraphy



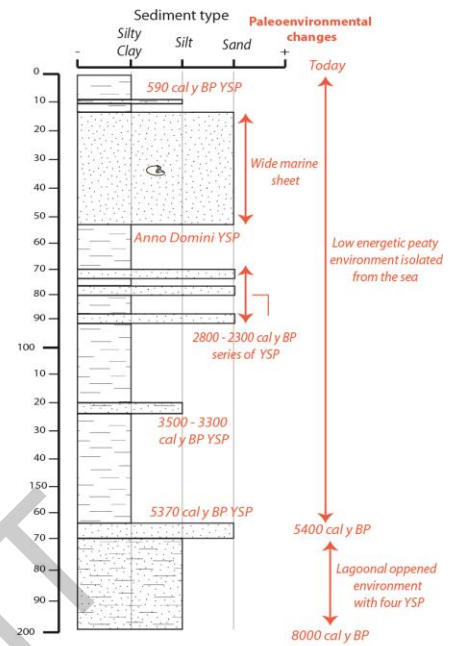
mean grain size (µm)	name of sample and measured Carbon-14 date	Silty Clay
organic matter (%)	<i>Bittium reticulatum</i> shell dated, datation not preserved for age depth modelling	Silt
Sediment composition (%)	SHELL*	Sand
clay	date cal y BP of disturbance estimated with age depth modeling	Pebble extracted
silt	6016	Layer containing marine shells
sand	series of storminess grouped into one stormy period	
geochemical signal of storminess		

Marais de la Guerche (YEU-MG)

Data obtained from sedimentary analyses



Interpretation of the lithostratigraphy

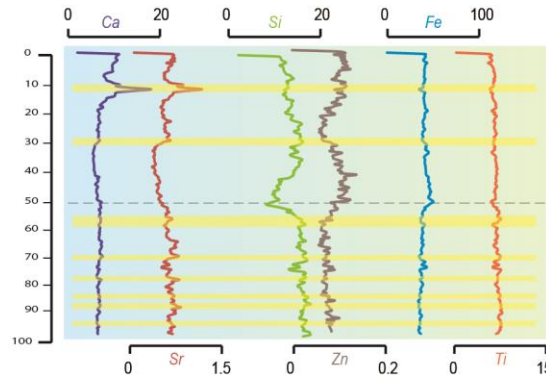
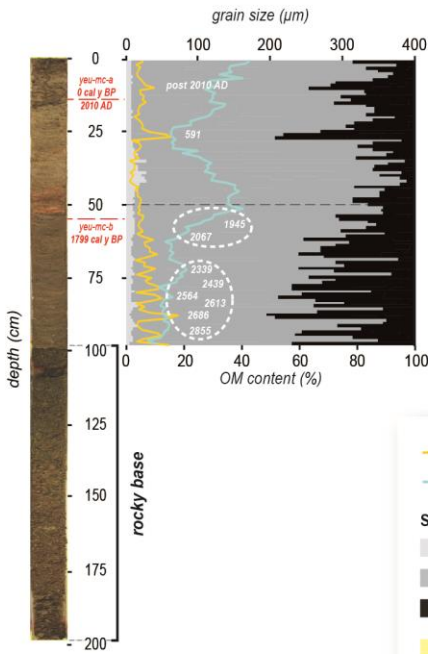


mean grain size (μm)	name of sample and measured Carbon-14 date	Silty Clay
organic matter (%)	<i>Bittium reticulatum</i> shell dated, datation not preserved for age depth modelling	Silt
Sediment composition (%)	SHELL* date cal y BP of disturbance estimated with age depth modeling	Sand
clay	5016 date cal y BP of disturbance estimated with age depth modeling	Pebble extracted
silt	series of storminess grouped into one stormy period	Layer containing marine shells
sand		
geochemical signal of storminess		

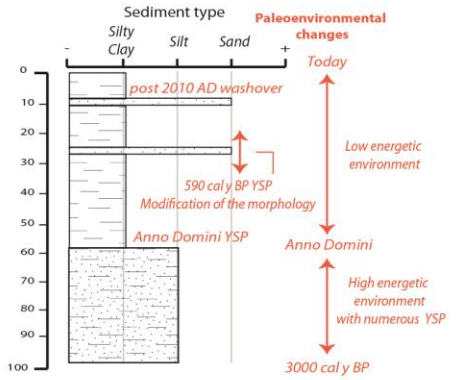
PREPRINT

Marais de la Croix (YEU-MC)

Data obtained from sedimentary analyses

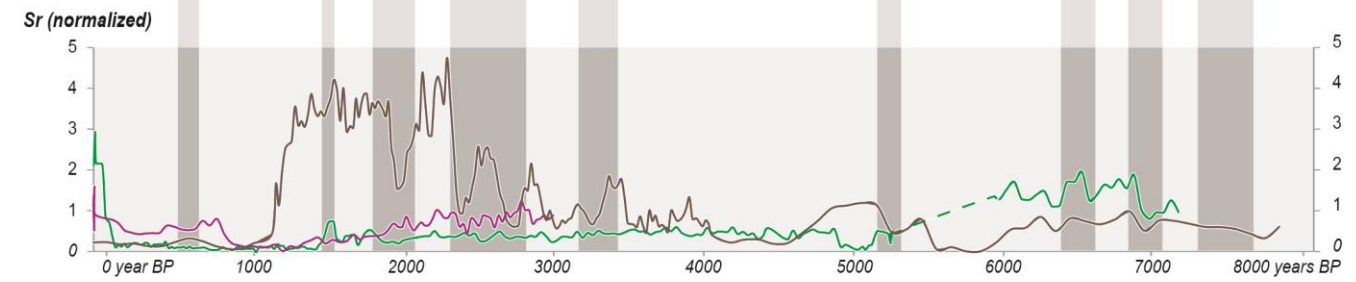
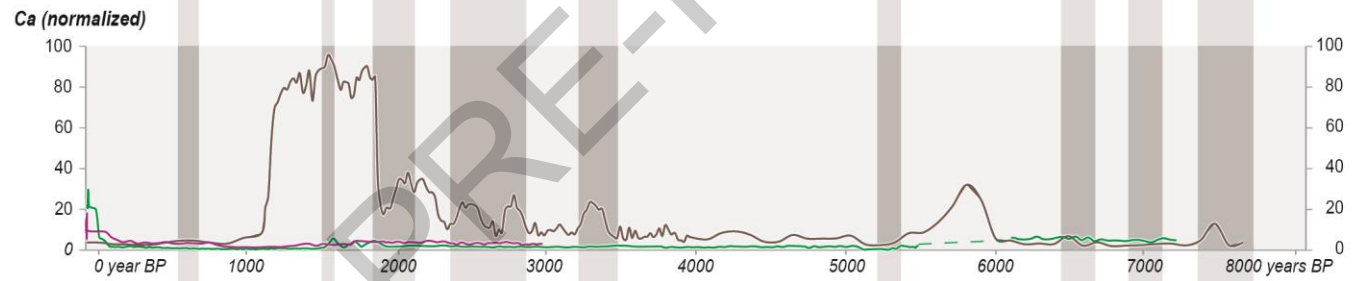
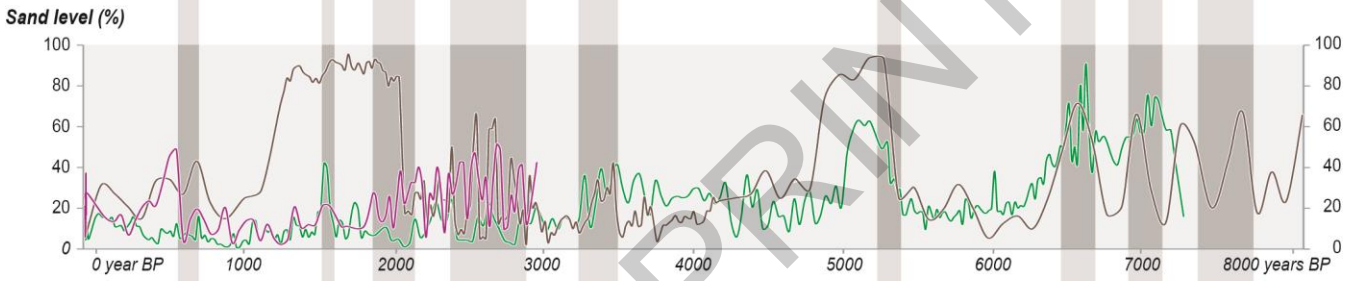
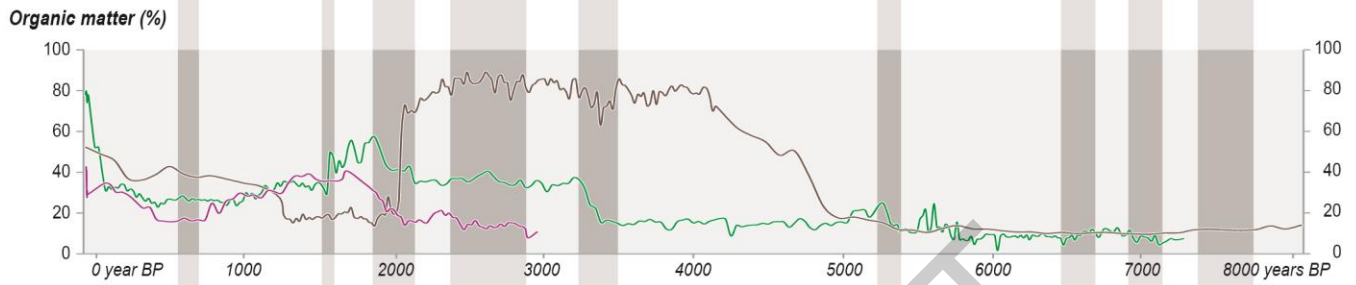
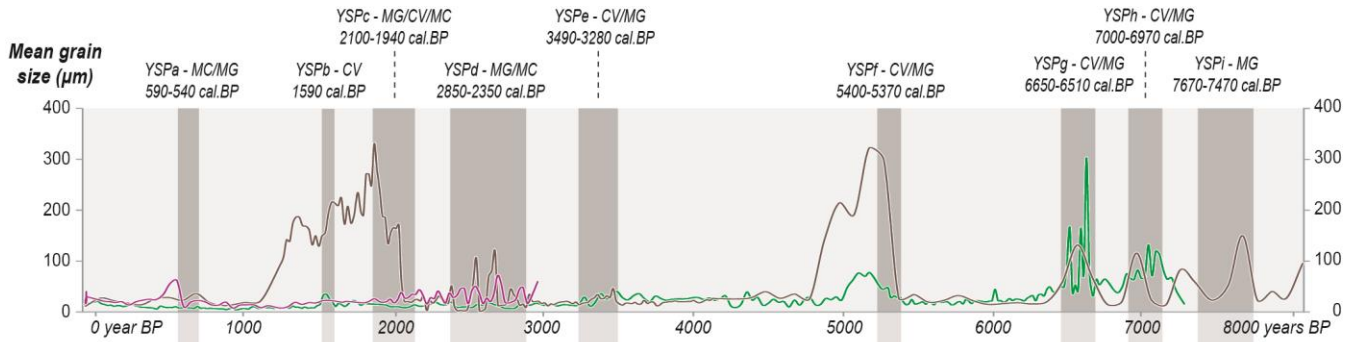


Interpretation of the lithostratigraphy



— mean grain size (μm)	yeu-mg-a name of sample and measured Carbon-14 date	Silty Clay
— organic matter (%)	860 cal y BP	Silt
Sediment composition (%)	<i>Bittium reticulatum</i> shell dated, datation not preserved for age depth modelling	Sand
clay	SHELL*	Pebble extracted
silt	6016 date cal y BP of disturbance estimated with age depth modeling	Layer containing marine shells
sand	series of storminess grouped into one stormy period	
geochemical signal of storminess		

PRE-PRINT



- Coulée Verte core (YEU-CV)
- Marais de la Guerche core (YEU-MG)
- Marais de la Croix core (YEU-MC)

■ You Stormy Period (YSP)

YSPa - MC/MG
540-590 cal.BP
Name, corresponding cores and
estimated date of the stormy period

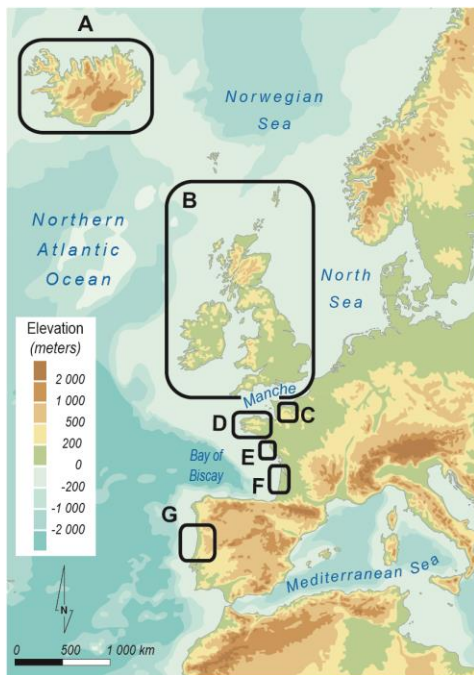


Figure 5. Proposition of European Atlantic Storm Events (EASEs) extracted from the comparison of existing European Atlantic storminess studies from sedimentary analysis :

- A : Iceland (Jackson et al., 2005) ;
- B : Britannic islands (Orme et al., 2016) ;
- C : Normandy (Sorrel et al., 2009) ;
- D : Brittany (Baltzer et al, 2014 & Van Vliet Lanoe et al., 2014) ;
- E : Western-central France (this paper) ;
- F : Aquitaine (Clarke et al., 2002) ;
- G : Central-Portugal (Clarke and Rendell, 2006).

Correlation of EASEs extracted from this work with :

- I : global high cold climatic periods (Wanner et al., 2011) determined from
- II : standardized ocean stacked Ice Rafted Debris records, with Bond's events numbered (Bond et al., 2001, 1997; Wanner et al., 2011)

Comparison with northern hemisphere storminess reviews :

- H : The Mediterranean Sea (Kaniewski et al., 2016)
- I : The North Sea (Jong et al., 2006)
- J : The Western Atlantic basin (Noren et al., 2002)
- K : The Eastern Pacific basin (Osleger et al., 2009)
- L : The Western Pacific basin (Zhu et al., 2017)

